Hindawi Publishing Corporation
Journal of Engineering
Volume 2014, Article ID 137426, 6 pages
http://dx.doi.org/10.1155/2014/137426

Research Article

Free Convection in Heat Transfer Flow over a Moving Sheet in Alumina Water Nanofluid

Padam Singh and Manoj Kumar

Department of Mathematics, Statistics and Computer Science, G.B. Pant University of Agriculture and Technology, Pantnagar, Uttarakhand 263145, India

Correspondence should be addressed to Padam Singh; tomar.padam@gmail.com

Received 24 May 2014; Accepted 4 October 2014; Published 2 November 2014

Academic Editor: Oronzio Manca

The present paper deals with study of free convection in two-dimensional magnetohydrodynamic (MHD) boundary layer flow of an incompressible, viscous, electrically conducting, and steady nanofluid. The governing equations representing fluid flow are transformed into a set of simultaneous ordinary differential equations by using appropriate similarity transformation. The equations thus obtained have been solved numerically using adaptive Runge-Kutta method with shooting technique. The effects of physical parameters like magnetic parameter, temperature buoyancy parameter on relative velocity and temperature distribution profile, shear stress profile, and temperature gradient profile were depicted graphically and analyzed. Significant changes were observed due to these parameters in velocity and temperature profiles.

1. Introduction

Applications of heat transfer through moving material in a moving fluid medium have wide range of applications in real world. Various researchers studied the concepts of moving sheet in a flowing fluid medium. Numerical and analytical solution for momentum and energy in laminar boundary layer flow over continuously moving sheet was discussed by Zheng and Zhang [1]. The authors found that the effect of velocity ratio parameter and other parameters on heat transfer were significant. Al-Sanea [2] studied the flow and thermal characteristic of a moving vertical sheet of extruded material close to and far downstream from the extrusion slot. Regimes of forced, mixed, and natural convection have been delineated, in buoyancy flow, as a function of Reynolds and thermal Grashof numbers for various values of Prandtl number and buoyancy parameter. Seddeek [3] analyzed the effect of magnetic field on the flow of micropolar fluid past a continuously moving plate. Patel et al. [4] suggested a new model for thermal conductivity of nanofluids which is found to agree excellently with a wide range of experimental published data. The momentum and heat transfer flow of an incompressible laminar fluid past a moving sheet based on composite reference velocity was studied by Cortell [5]. The author found that the direction of the wall shear stress changes in such an interval and an increase of the relative velocity parameter yields an increase in temperature. Ishak et al. [6] studied the magnetohydrodynamic boundary layer flow due to a moving extensible surface. It was found that the dual solutions exist for the flow near y-axis, where the velocity profiles show a reversed flow. Bachok et al. [7] investigated steady, laminar boundary layer flow of a nanofluid past a moving semi infinite flat plate. The results indicate that dual solutions exist when the plate and the free stream move in the opposite directions. Habib and El-Zahar [8] proposed a model for determining the heat transfer between a moving sheet and flowing fluid. The authors found that the heat transfer depends on the relative velocity between the moving fluid and the moving sheet to certain values. Energy conversion for conjugate convection, conduction, and radiation analysis have been performed for free convective heat transfer with radiation by Hsiao [9]. The results show that the free convection effect will produce a larger heat transfer effect better than the forced convection. Raguraman et al. [10] investigated the effects of some important design parameters for coal-water slurry in agitated vessel used in coal gasification such as stirrer speed, location of stirrer, D/d ratio, and coal-water ratio. Confirmation test verified that the Taguchi method achieved optimization of heat transfer coefficient in agitated vessel. The objective of the present study is to analyze the effect of magnetic field and temperature buoyancy effect on the heat transfer flow between a moving sheet and moving alumina water nanofluid environment. Hsiao [11, 12] studied two-dimensional conjugate heat transfer with Ohmic dissipation mixed convection of an incompressible Maxwell fluid on a stagnation point and also investigated energy conversion problems of conjugate conduction, convection, and radiation heat and mass transfer with viscous dissipation and magnetic effects. The results have shown that it should produce greater heat transfer effect with larger values of Prandtl number, free convection parameter, and conduction-convection number. On the other hand, the Eckert number and magnetic parameter will reduce the heat transfer effect. For heat convection energy conversion aspect, some importance parameters applied to the system, such as buoyancy parameters, radiative energy parameter, boundary proportional parameter, and Prandtl number which can produce positive effects for larger values of those parameters. Idusuyi et al. [13] formulated a computational model for the heat generation and dissipation in a disk brake during braking and the following release period. The results show similarity in thermal behaviour at the contact surface for the asbestos and aramid brake pad materials with a temperature difference of 1.8 K after 10 seconds.

The objective of the present study is to analyze the effect of magnetic field and temperature buoyancy effect on the heat transfer flow between a moving sheet and moving alumina water nanofluid environment.

2. Mathematical Description

The graphical model of the problem considered has been given to depict the flow configuration and coordinate system. The system deals with two-dimensional MHD boundary layer, incompressible, viscous, electrically conducting, and steady fluid flow (Figure 1). The governing equations representing flow are the following:

$$\frac{\partial u}{\partial x} + \frac{\partial v}{\partial y} = 0 \tag{1}$$

$$\begin{aligned} u\frac{\partial u}{\partial x} + v\frac{\partial u}{\partial y} &= -\frac{1}{\rho_{\text{nf}}}\frac{\partial p}{\partial x} + \upsilon_{\text{nf}}\frac{\partial^2 u}{\partial y^2} \\ &\quad + g\left(\beta_T\right)_{\text{nf}}\left(T - T_\infty\right) - \frac{\sigma_{\text{nf}} B^2(x)}{\rho_{\text{nf}}} u \end{aligned} \tag{2}$$

$$u\frac{\partial T}{\partial x} + v\frac{\partial T}{\partial y} = \alpha_{\text{nf}}\frac{\partial^2 T}{\partial y^2}, \tag{3}$$

where u and v are the velocity components in x and y direction, respectively, υ_{nf}, $(\beta_T)_{\text{nf}}$, ρ_{nf}, σ_{nf}, and α_{nf} are the kinematic viscosity, thermal expansion coefficient, density, electrical conductivity, and thermal diffusivity of the nanofluid.

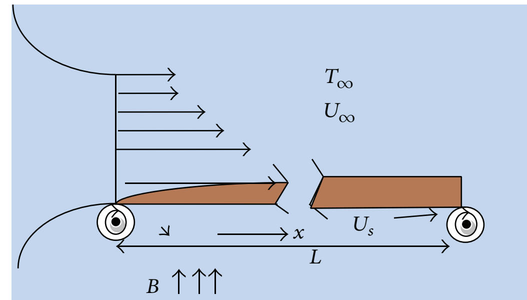

Figure 1: Flow configuration and coordinate system.

g is the gravitational acceleration and T, T_w, and T_∞ are the temperature of the nanofluid inside the thermal boundary layer, the plate temperature, and the nanofluid temperature at free stream, respectively. $B(x) = (1/\sqrt{x})B_0$ denotes the magnetic field imposed in the transverse direction to the fluid.

The appropriate boundary conditions for the abovementioned problem are as follows (Table 1):

$$\begin{aligned} &u = U_s, \quad v = 0, \quad T = T_s, \quad \text{at } y = 0, \\ &u \longrightarrow U_\infty, \quad T \longrightarrow T_\infty, \quad \text{as } y \longrightarrow \infty. \end{aligned} \tag{4}$$

3. Method for Solution

To solve the governing equations (1), (2), and (3) with the boundary conditions (4), the following similarity transformation has been introduced:

$$\begin{aligned} \psi &= \left[\upsilon_{\text{nf}}\left(U_\infty - U_s\right)x\right]^{1/2} f(\eta), \\ \theta &= \frac{T - T_\infty}{T_s - T_\infty}, \quad \eta = \left[\frac{U_\infty - U_s}{\upsilon_{\text{nf}} x}\right]^{1/2} y. \end{aligned} \tag{5}$$

Here U_∞ and U_s are free stream velocity and moving sheet velocity, respectively. ψ is the stream function which satisfies (1) with $u = \partial\psi/\partial y$ and $v = -\partial\psi/\partial x$. Thus, (5) gives

$$\begin{aligned} u &= \left(U_\infty - U_s\right) f'(\eta), \\ v &= -\frac{1}{2}\left(\frac{\upsilon_{\text{nf}}\left(U_\infty - U_s\right)}{x}\right)^{1/2}\left(f(\eta) - \eta f'(\eta)\right). \end{aligned} \tag{6}$$

Now using (5) and (6) in (2) and (3), we get the following nonlinear differential equations:

$$\begin{aligned} f'''(\eta) + \frac{1}{2} f(\eta) f''(\eta) - M f'(\eta) + g_t \theta(\eta) &= 0 \\ \theta'' + \frac{1}{2}\Pr f(\eta)\theta'(\eta) &= 0; \end{aligned} \tag{7}$$

Table 1: Nanofluid properties.

Dynamic viscosity [14]	$\mu_{nf} = \mu_f/(1-\emptyset)^{2.5}$
Density [15]	$\rho_{nf} = (1-\emptyset)\,\rho_f + \emptyset\rho_s$
Specific heat capacity [16]	$\left(C_p\right)_{nf} = (1-\emptyset)\left(C_p\right)_f + \emptyset\left(C_p\right)_s$
Thermal conductivity [4]	$\dfrac{(k_s/k_f) + (n-1) - \emptyset(1-(k_s/k_f))k_{nf}}{= k_f(k_s/k_f) + (n-1) - (n-1)\,\emptyset(1-(k_s/k_f))}$
Kinematic viscosity [17]	$\upsilon_{nf} = \mu_{nf}/\rho_{nf}$
Thermal diffusivity	$\alpha_{nf} = k_{nf}/\rho_{nf}\left(C_p\right)_{nf}$
Empirical shape factor	$n = 3/\psi$, $\psi = 1$ for spherical particles

the boundary conditions (4) will become

$$
\begin{gathered}
f(0) = 0, \qquad f'(0) = \frac{1}{|1-\alpha|}, \\
f''(0) = \text{unknown}, \qquad \theta(0) = 1, \\
\theta'(0) = \text{unknown}, \\
f'(\eta) \longrightarrow \frac{\alpha}{|1-\alpha|}, \qquad \theta(\eta) \longrightarrow 0, \quad \text{as } \eta \longrightarrow \infty,
\end{gathered}
\tag{8}
$$

where $\alpha = 0$ represent the state of moving surface in stationary fluid ($U_\infty = 0$) and $0 < \alpha < \infty$ is the condition of moving surface in moving fluid with $U_\infty > U_s$. The dimensionless parameters introduced in (7) are defined as follows.

$M = \sigma_{nf}B_0^2/\rho_{nf}(U_\infty - U_s)$ is the magnetic parameter, $G_r = g\,(\beta_T)_{nf}\,(T_s - T_\infty)\,x^3/\upsilon_{nf}^2$ is the local temperature Grashof number, $\mathrm{Re} = U_\infty x/\upsilon_{nf}$ is the local Reynolds number, $g_t = G_r/\mathrm{Re}^2$ is the temperature buoyancy parameter, $\mathrm{Pr} = \upsilon_{nf}/\alpha_{nf}$ is the Prandtl number, and $\alpha = U_\infty/U_s$ is the relative velocity parameter.

To solve the set of nonlinear differential equations (7) with subject to the boundary conditions (8), adaptive Runge-Kutta method with shooting technique has been applied. This method is based on the discretization of the problem domain and the calculation of unknown boundary conditions. The domain of the problem is discretized and the boundary conditions for $\eta = \infty$ are replaced by $f'(\eta_{\max}) = \alpha/\mathrm{abs}(1-\alpha)$, and $\theta(\eta_{\max}) = 0$ where $\eta_{\max}$ is sufficiently large value of η comparing to step size at which the boundary conditions (8) for $f'(\eta)$ and $\theta(\eta)$ are satisfied. On account of the consistency and to fulfill stability criteria $\eta_{\max} = 10$ and step size $\Delta\eta = 0.01$ have been taken. To solve the problem the nonlinear equations (7) are first converted into first order ordinary linear differential equations as follows:

$$
\begin{gathered}
f'(\eta) = y(2); \qquad f''(\eta) = y(3); \\
f'''(\eta) = \left[-\frac{1}{2}y(1)\,y(3) + My(2) - g_t y(4)\right]; \\
\theta' = y(5); \qquad \theta''(\eta) = \left[-\frac{1}{2}\,\mathrm{Pr}\,y(1)\,y(5)\right].
\end{gathered}
\tag{9}
$$

Table 2: Values of $f''(0)$ and $\theta'(0)$ for $\mathrm{Pr} = 6.6556406$ and $\emptyset = 0.05$ obtained by shooting method.

Magnetic parameter (M)	Temperature buoyancy parameter (g_t)	Wall shear stresses $f''(0)$	Skin friction coefficient $\theta'(0)$
0.0	0.2	−0.664300	−1.97611
0.2	0.0	−1.297800	−1.90991
0.2	0.5	−1.157890	−1.91991
0.2	1.0	−1.016890	−1.92921
0.2	3.0	−0.479190	−1.96421
0.5	0.2	−1.768590	−1.85411
1.0	0.2	−2.269990	−1.79411
3.0	0.2	−3.605449	−1.65431

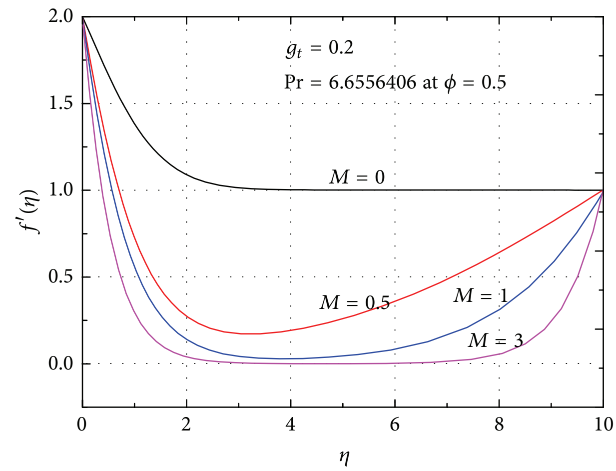

Figure 2: Effect of magnetic parameter on velocity.

There are three conditions on the boundary $\eta = 0$ and two conditions at $\eta = \infty$ as given in (8). Shooting technique has been used to find required missing initial conditions. The value of unknowns $f''(0)$ and $\theta'(0)$ has been tabulated in Table 2. Adaptive Runge-Kutta method estimates the truncation error at each integration step and automatically adjusts the step size to keep the error within prescribed limits. The formula used to measure the actual conservative error is defined by $e(h) = \left((1/5)\sum_{i=1}^{5} E_i^2(h)\right)^{1/2}$; here $E_i(h)$ is the measure of error in the dependent variable y_i. Per-step error control is achieved by adjusting the increment h by $h_{i+1} = 0.9h_i(\varepsilon/e(h_i))^{1/5}$, $i = 1, 2, 3, 4, 5$, so that it is approximately equal to the prescribed tolerance $\varepsilon = 10^{-6}$. The assumed initial step size is $h = 0.01$.

4. Result and Discussion

The computations have been made for velocity, shear stress, concentration, and concentration gradient profiles corresponding to fixed values of magnetic parameter (M), α, and temperature buoyancy parameter (g_t). The value of $\mathrm{Pr} = 6.6556406$ is taken corresponding to 0.05 volume fraction of the alumina water nanofluid at 20°C. The parameter g_t has been introduced to represent the temperature buoyancy effect on flow field. Figures 2–6 exhibit the velocity, shear stress,

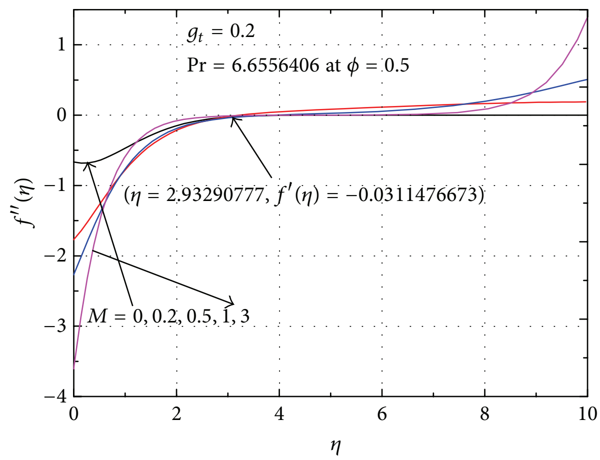

Figure 3: Effect of magnetic parameter on shear stress.

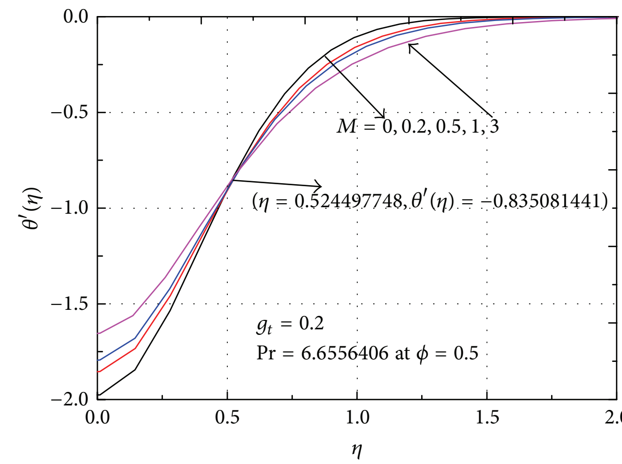

Figure 5: Effect of magnetic parameter on temperature gradient.

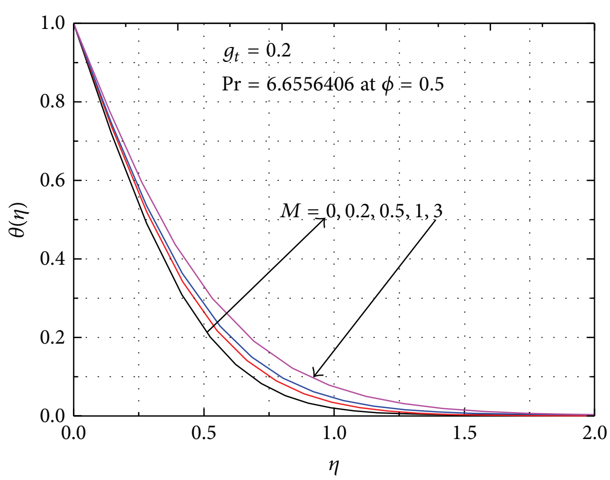

Figure 4: Effect of magnetic parameter on temperature.

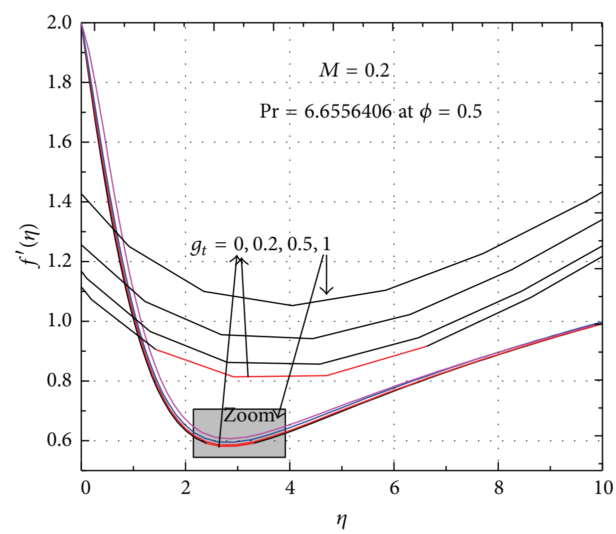

Figure 6: Effect of temperature buoyancy parameter on velocity.

concentration, and concentration gradient profiles, respectively, for various values of magnetic parameter (i.e., $M = 0, 0.2, 0.5, 1, 3$). It is noticed that in Figures 2 and 3 that the velocity decreases and the shear stress decreases up to (2.93290777, −0.0311476673) and then increases with an increase in the magnetic parameter. The temperature increases with an increase in the magnetic parameter; temperature gradient increases up to (0.524497748, −0.835081441) and then decreases with an increment in the values of magnetic parameter as shown in Figures 4 and 5. Figures 6 and 7 show the effect of convection parameter on velocity, shear stress, concentration, and concentration gradient profiles, respectively, for $g_t = 0, 0.2, 0.5, 1$. It has been observed that the velocity increases with an increase in the convection parameter as shown in Figure 6, and shear stress increases up to (0.433856945, −1.03343467) with an increase in the convection parameter and then decreases as shown in Figure 7. The effect of convection parameter on temperature gradient and temperature also has been studied through Figures 8 and 9. It is noticed that the temperature and temperature gradient

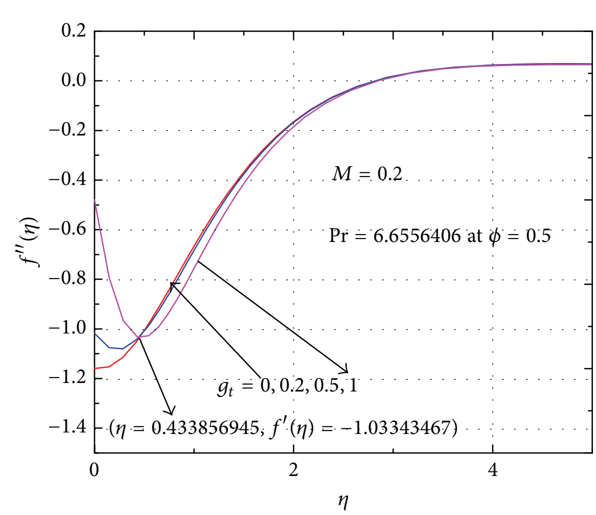

Figure 7: Effect of temperature buoyancy parameter on shear stress.

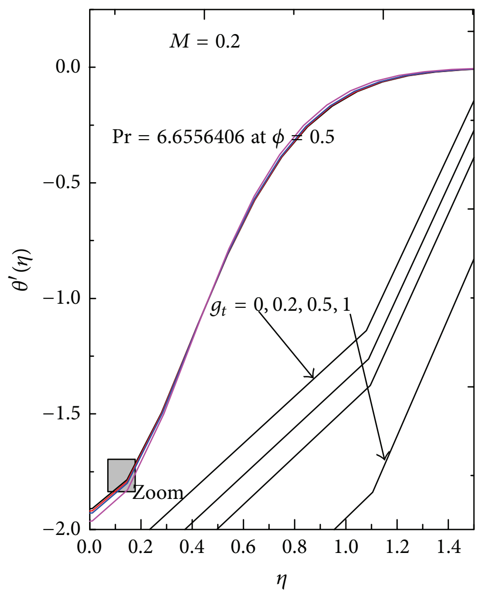

FIGURE 8: Effect of temperature buoyancy parameter on temperature gradient.

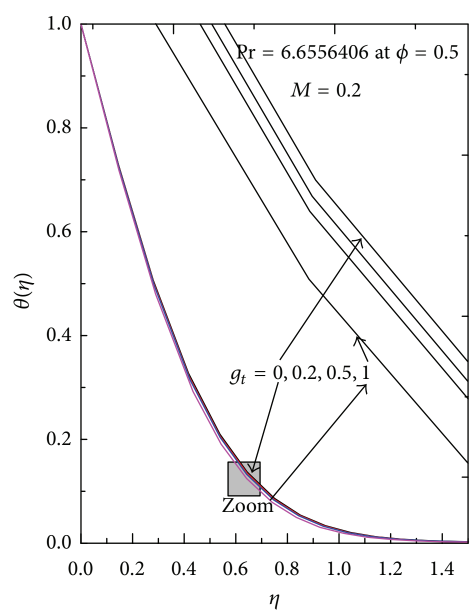

FIGURE 9: Effect of temperature buoyancy parameter on temperature.

show significant changes with an increase in the temperature buoyancy parameter.

5. Conclusion

Free convective heat transfer in an electronically conducting nanofluid over a moving sheet with magnetic field is considered. The nonlinear partial differential equations are transformed into a system of nonlinear ordinary differential equations by using similarity transformation and then solved numerically using the Runge-Kutta fifth order method along with the shooting technique. From the numerical calculations of the skin friction coefficient and wall shear stresses the following is concluded.

(i) An increase in magnetic parameter decreases the velocity and wall shear stress but enhances the temperature, skin friction coefficient. The shear stress decrease up to a fixed value of magnetic parameter and after that goes to increases. For the magnetic parameter, temperature gradient shows the opposite behaviour to the shear stress.

(ii) As the temperature buoyancy parameter increases, it increases the velocity, wall shear stress and decreases skin friction coefficient and temperature gradient.

Conflict of Interests

The authors declare that there is no conflict of interests regarding the publication of this paper.

References

[1] L. C. Zheng and X. X. Zhang, “Skin friction and heat transfer in power-law fluid laminar boundary layer along a moving surface,” *International Journal of Heat and Mass Transfer*, vol. 45, no. 13, pp. 2667–2672, 2002.

[2] S. A. Al-Sanea, “Convection regimes and heat transfer characteristics along a continuously moving heated vertical plate,” *International Journal of Heat and Fluid Flow*, vol. 24, no. 6, pp. 888–901, 2003.

[3] M. A. Seddeek, “Flow of a magneto-micropolar fluid past a continuously moving plate,” *Physics Letters, Section A: General, Atomic and Solid State Physics*, vol. 306, no. 4, pp. 255–257, 2003.

[4] H. E. Patel, T. Sundararajan, T. Pradeep, A. Dasgupta, N. Dasgupta, and S. K. Das, “A micro-convection model for thermal conductivity of nanofluids,” *Pramana—Journal of Physics*, vol. 65, no. 5, pp. 863–869, 2005.

[5] R. Cortell, “Flow and heat transfer in a moving fluid over a moving flat surface,” *Theoretical and Computational Fluid Dynamics*, vol. 21, no. 6, pp. 435–446, 2007.

[6] A. Ishak, R. Nazar, and I. Pop, “MHD boundary-layer flow due to a moving extensible surface,” *Journal of Engineering Mathematics*, vol. 62, no. 1, pp. 23–33, 2008.

[7] N. Bachok, A. Ishak, and I. Pop, “Boundary-layer flow of nanofluids over a moving surface in a flowing fluid,” *International Journal of Thermal Sciences*, vol. 49, no. 9, pp. 1663–1668, 2010.

[8] H. M. Habib and E. R. El-Zahar, “Mathematical modeling of heat-transfer for a moving sheet in a moving fluid,” *Journal of Applied Fluid Mechanics*, vol. 6, no. 3, pp. 369–373, 2013.

[9] K.-L. Hsiao, “Energy conversion conjugate conduction-convection and radiation over non-linearly extrusion stretching sheet with physical multimedia effects,” *Energy*, vol. 59, pp. 494–502, 2013.

[10] C. M. Raguraman, A. Ragupathy, and L. Sivakumar, “Experimental determination of heat transfer coefficient in stirred vessel for coal-water slurry based on the taguchi method,” *Journal of Engineering*, vol. 2013, Article ID 719296, 8 pages, 2013.

[11] K.-L. Hsiao, "Conjugate heat transfer for mixed convection and Maxwell fluid on a stagnation point," *Arabian Journal for Science and Engineering*, vol. 39, no. 6, pp. 4325–4332, 2014.

[12] K.-L. Hsiao, "Nanofluid flow with multimedia physical features for conjugate mixed convection and radiation," *Computers & Fluids*, vol. 104, pp. 1–8, 2014.

[13] N. Idusuyi, I. Babajide, O. K. Ajayi, and T. T. Olugasa, "A computational study on the use of an aluminium metal matrix composite and aramid as alternative brake disc and brake pad material," *Journal of Engineering*, vol. 2014, Article ID 494697, 6 pages, 2014.

[14] A. Einstein, *Investigation on the Theory of the Brownian Movement*, Dover, New York, NY, USA, 1956.

[15] D. A. Drew and S. L. Passman, *Theory of Multicomponent Fluids*, Springer, New York, NY, USA, 1999.

[16] Y. Xuan and W. Roetzel, "Conceptions for heat transfer correlation of nanofluids," *International Journal of Heat and Mass Transfer*, vol. 43, no. 19, pp. 3701–3707, 2000.

[17] E. Mamut, "Characterization of heat and mass transfer properties of nanofluids," *Romanian Journal of Physics*, vol. 51, pp. 5–12, 2006.